Available online at www.sciencedirect.com
ScienceDirect
Journal of Organometallic Chemistry 692 (2007) 5383–5389
Journal of Organometallic Chemistry
www.elsevier.com/locate/jorganchem

Theoretical study of the strong intramolecular hydrogen bond and metal–ligand interactions in group 10 (Ni, Pd, Pt) bis(dimethylglyoximato) complexes

Attila Kovács *

Materials Structure and Modeling Research Group of the Hungarian Academy of Sciences, Budapest University of Technology and Economics, H-1111 Budapest, Szt. Gellért tér 4, Hungary

Received 29 January 2007; received in revised form 9 August 2007; accepted 23 August 2007
Available online 28 August 2007

Abstract

The structural and bonding characteristics of the bis(dimethylglyoximato) complexes of group 10 transition metals ([M(*dmg*)$_2$], where M = Ni, Pd and Pt) were investigated by means of quantum chemical computations. The equilibrium geometries, energetic and bonding properties were computed using the B3P86 exchange-correlation density functional in conjunction with a 6-311+(+)G** basis set. The computations revealed that the strong O$^-\cdots$H–O hydrogen bond exists only in the presence of the metal cations. The free (*dmg*)$_2^{2-}$ ligand has significantly different geometry in which the O$^-\cdots$H–O interaction is replaced by N$\cdots$O–H bonds. The characteristics of the metal–ligand interactions were determined by natural bond orbital analysis.

Keywords: Transition metal complexes; Hydrogen bonding; Charge transfer interactions; DFT computations; Natural bond orbital analysis

1. Introduction

The bis(dimethylglyoximato) complexes of group 10 transition metals, [M(*dmg*)$_2$], where M = Ni, Pd and Pt, are best known about their analytical application for the gravimetric determination of these metal ions [1,2]. This gravimetric determination is facilitated by the very strong metal–ligand interaction resulting in an insoluble precipitate in water. Dissolving the precipitates in appropriate solvents makes also a spectrophotometric determination of the metal ions possible [3]. More recent application of the complexes appeared as precursors for deposition of thin metal films by MOCVD [4–6]. The complexes are also promising candidates for third-order non-linear optical materials [7–12]. This is due to their crystal structure in which the planar complexes are arranged face-to-face upon each other resulting in close metal–metal contacts. Thus one-dimensional alloys with unique optoelectric properties could be prepared.

The [M(*dmg*)$_2$] complexes are very interesting also from a structural point of view. The strong metal–ligand bond is revealed by the very short Ni–N, Pd–N and Pt–N distances (1.86 [13], 1.96 [14] and 1.98 Å [15], respectively), being below the sum of covalent radii of the bonded atoms (1.96, 2.06 and 2.03 Å [16], respectively). The above X-ray diffraction studies pointed also out the close O$\cdots$O inter-*dmg* distances in the complexes (2.46 [13], 2.63 [14] and 2.64 Å [15], respectively) indicative of very strong intramolecular hydrogen bonding interactions. These strong hydrogen bonds were justified by the strongly red-shifted OH stretching bands in the IR spectra [17–24]. As the [M(*dmg*)$_2$] complexes consist formally of M^{2+} and (*dmg*)$_2^{2-}$ ions, the strong inter-*dmg*$^-$ hydrogen bonds were explained by the anionic character of the acceptor oxygen in *dmg*$^-$. This model, however, could not explain the

* Address: Department of Inorganic and Analytical Chemistry, Budapest University of Technology and Economics, H-1111 Budapest, Szt. Gellért tér 4, Hungary. Tel.: +36 1 463 2278; fax: +36 1 463 3408.
E-mail address: akovacs@mail.bme.hu

0022-328X/$ - see front matter © 2007 Elsevier B.V. All rights reserved.
doi:10.1016/j.jorganchem.2007.08.024

differences in the three complexes: the considerably shorter hydrogen bond in [Ni(*dmg*)$_2$] with respect to [Pd(*dmg*)$_2$] and [Pt(*dmg*)$_2$] (*vide supra* the O···O distances), which difference was supported by the IR spectral characteristics.

Previous structural studies of the title [M(*dmg*)$_2$] complexes include several X-ray investigations [13–15,25–27]. The strong intramolecular hydrogen bond has been investigated mainly by vibrational spectroscopy [17–23,28]. Previous theoretical investigations of the title complexes included a Hartree–Fock-based static exchange approximation study [29] as well as a DFT transition potential approach [30] used for the interpretation of the photoabsorption spectra of [Ni(*dmg*)$_2$]. Our recent joint experimental and theoretical study of [Ni(*dmg*)$_2$] focused on the vibrational properties of the complex performing a complete normal coordinate analysis on the basis of a scaled quantum mechanical force field [24]. Neither detailed geometry or bonding data have been reported in the above papers.

In spite of the numerous structural and spectroscopic studies several questions are still open about the bonding interactions in the title complexes. Is the anionic character of the glyoximato oxygen the real reason of the strong hydrogen bonds? What is the relation between the hydrogen bonding and donor–acceptor interactions in the complexes? Why are the hydrogen bonds between the Ni and Pd/Pt complexes so different? How large is the barrier of the proton exchange in these asymmetric hydrogen bonds? What are the characteristics of the metal–ligand interactions in the complexes?

In the present study we aim to answer these questions using quantum chemical calculations. We computed the equilibrium structures of the three complexes as well as the symmetric transition states. We evaluated the energies of complex formation, while the computations on the free $(dmg)_2^{2-}$ ligand revealed the nature of the hydrogen bonding interaction in the absence of the complexing metal. A quantitative analysis of the metal–ligand interactions was performed by natural bond orbital (NBO) [31] analysis.

2. Computational details

Preliminary studies of the possible conformers (methyl rotamers) were performed using the B3LYP exchange-correlation functional [32,33] in conjunction with the relativistic effective core potential (RECP) of Hay and Wadt for the metals [34] and the 6-31G(d,p) basis set for the other elements. For more accurate calculations on the found global minima we increased the basis set for the main group elements to 6-311+G(d) and that of the hydrogens to 6-311G(p). A single set of diffuse functions was additionally applied on the hydroxyl hydrogens for a better description of the hydrogen bonding interaction they are involved in. The valence basis set of the metals (Ni: 341/311/41; Pd: 341/321/31; Pt: 341/321/21) [34] was extended by *f* polarization functions ($\alpha_{Ni} = 3.130$; $\alpha_{Pd} = 1.472$; $\alpha_{Pt} = 0.993$ [35]). This basis is denoted as 6-311+(+)G** throughout the paper. We carried out test calculations at the B3LYP/6-311+(+)G** and B3P86/6-311+(+)G** [32,36] levels in order to verify which exchange-correlation density functional performs better for the title complexes. We compared the computed geometrical parameters with available experimental data. The agreement for the M–N distances and the hydrogen bonding moiety was better in the case of the B3P86/6-311+(+)G** level, hence we selected this level for the overall study. The characters of the stationary points were always checked by frequency calculations at the levels of the geometry optimizations. The dissociation energies were corrected for BSSE using the counterpoise method [37] and for zero-point vibrational energy obtained at the B3P86/6-311+(+)G** level. The geometry optimizations and the frequency and BSSE calculations were carried out with the GAUSSIAN 03 [38] program package. The natural bond orbital analyses [31] were performed using the NBO 5.0 code [39] in conjunction with the GAUSSIAN 98 [40] program. The computed structures were visually analysed by the Molden 3.8 program [41].

3. Results and discussion

3.1. Molecular geometries

The crystal structure of the title [M(*dmg*)$_2$] complexes is known from X-ray diffraction investigations (Ni [13], Pd [14], Pt [15]). These studies concluded on molecular geometries of C_{2h} symmetry [13–15]. On that basis, and in order to gain from the selection rules, our recent vibrational analysis of solid [Ni(*dmg*)$_2$] has been performed using a C_{2h} reference geometry [24].

The computed geometries of the title [M(*dmg*)$_2$] complexes are depicted in Fig. 1. Note that in the present geometry optimizations no symmetry constrains were applied. The obtained structures are slightly asymmetric because of the steric interactions of the methyl groups with the oxygen lone pairs. A survey of different methyl rotamers with C_s and C_{2h} global molecular symmetry indicated the saddle-point character of these symmetric structures with two or four imaginary frequencies. Note that the energy differences between the global minima and the C_{2h} structures are very small (below 1 kJ/mol), and the geometrical parameters of the bis(glyoximato)-metal skeleton show only negligible differences.

The geometry optimizations resulted in different stable relative orientations of the methyl groups in the Ni and Pd/Pt complexes: in [Ni(*dmg*)$_2$] a staggered relative orientation of the facing methyl groups while in [Pd(*dmg*)$_2$] and [Pt(*dmg*)$_2$] a distorted (by ca. 15°) eclipsed one is preferred (cf. Fig. 1). Inspection of the computed bond angles revealed somewhat smaller C_4–C_5–$C_{5'}$ and C_5–C_4–$C_{4'}$ angles in the [Pd(*dmg*)$_2$] and [Pt(*dmg*)$_2$] complexes than in [Ni(*dmg*)$_2$] (cf. Table 1), indicating larger steric interactions between the methyls in the former complexes. In [Ni(*dmg*)$_2$], the *dmg* ligand has to bend more in order to accommodate to the (smaller) radius of Ni. This results in smaller N_3–C_4–C_5 and C_4–C_5–N_6 angles allowing larger

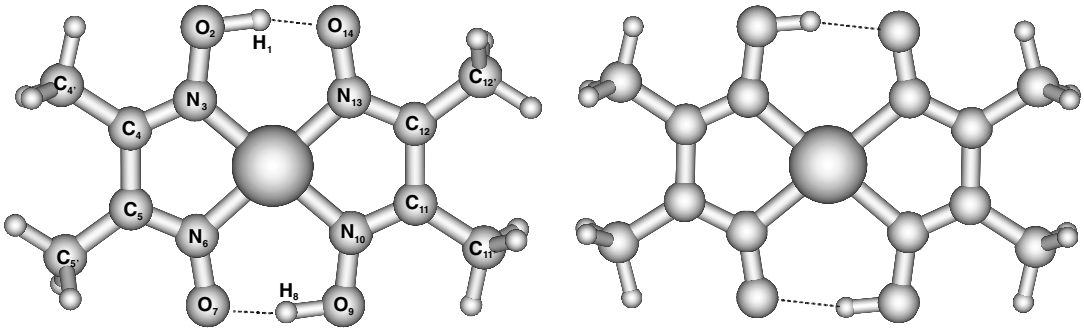

Fig. 1. Optimized geometries of the [M(*dmg*)$_2$] complexes from B3P86/6-311+(+)G** calculations.

Table 1
Selected (experimental and computed) geometrical parameters[a] of the [M(*dmg*)$_2$] complexes (M = Ni, Pd, Pt)

	[Ni(*dmg*)$_2$]		[Pd(*dmg*)$_2$]		[Pt(*dmg*)$_2$]	
	Exp.[b]	B3P86	Exp.[c]	B3P86	Exp.[d]	B3P86
$M–N_3$	1.862(3)	1.873	1.967(3)	1.989	1.976(12)	1.976
$M–N_6$	1.859(3)	1.894	1.962(3)	2.000	1.995(13)	1.994
$N_3–O_2$	1.350(40)	1.338	1.352(4)	1.349	1.354(24)	1.351
$N_6–O_7$	1.341(4)	1.288	1.322(4)	1.275	1.351(18)	1.279
$O_2–H_1$	1.109	1.050		1.014	1.06(15)	1.014
$O_2\cdots O_{14}$	2.457(4)	2.477	2.626(5)	2.669	2.638(19)	2.666
$H_1\cdots O_{14}$	1.354	1.442		1.671	1.63(15)	1.667
$N_3–C_4$	1.291(5)	1.294	1.280(4)	1.295	1.282(29)	1.299
$C_4–C_5$	1.467(5)	1.462	1.472(4)	1.467	1.425(29)	1.461
$C_5–N_6$	1.292(5)	1.305	1.299(4)	1.314	1.308(24)	1.316
$C_4–C_{4'}$	1.489(5)	1.487	1.489(4)	1.489	1.510(30)	1.487
$C_5–C_{5'}$	1.481(5)	1.486	1.487(4)	1.489	1.467(31)	1.487
$N_3–M–N_6$	82.4	83.0	79.9(1)	80.0	78.2(7)	79.5
$N_6–M–N_{10}$	97.6	97.0	100.2(1)	100.0	101.8(7)	100.5
$M–N_3–C_4$	116.3	115.4	116.3(2)	115.6	116.8(14)	116.4
$M–N_6–C_5$	116.6	114.8	115.7(2)	114.8	115.9(12)	115.4
$N_3–O_2–H_1$	101.5	103.3		103.4	111.9(80)	103.6
$C_4–N_3–O_2$	119.9	120.3	121.8(3)	121.6	123.2(15)	121.1
$C_5–N_6–O_7$	119.5	121.7	123.0(3)	125.2	125.0(14)	124.6
$O_2–H_1\cdots O_{14}$	172.1	167.0		167.3	159(13)	167.4
$N_{13}–O_{14}\cdots H_1$	101.1	104.3		106.3		106.0
$C_5–C_4–N_3$	112.5	113.5	114.1(3)	115.1	115.3(19)	114.6
$C_4–C_5–N_6$	112.2	113.3	114.0(3)	114.6	113.9(18)	114.0
$C_5–C_4–C_{4'}$	124.3	123.2	123.5(3)	122.2	124.1(19)	122.8
$C_4–C_5–C_{5'}$	125.0	125.5	124.7(3)	123.6	126.6(19)	124.1

[a] Bond distances are given in angstrom, bond angles in degrees. For the numbering of atoms see Fig. 1. The computed data were obtained at the B3P86/6-311+(+)G** level.
[b] From Ref. [13]. Part of the data were obtained from the cif file.
[c] From Ref. [14].
[d] From Ref. [15].

$C_4–C_5–C_{5'}$ and $C_5–C_4–C_{4'}$ ones. Note that the position of the methyl hydrogens has been determined in the X-ray studies of [Ni(*dmg*)$_2$] [13] and [Pt(*dmg*)$_2$] [15], where eclipsed arrangements of the facing methyl groups were found. The small energy required for a rotation of the methyl can be covered easily by packing effects in the crystal, explaining the disagreement of the present computed and experimental observation on [Ni(*dmg*)$_2$].

Selected computed geometrical parameters are compared with the experimental ones in Table 1. In agreement with the experimental structural data, the computations reproduced the strong asymmetric O–H$\cdots$O intramolecular hydrogen bonds, the very similar lengths of the $M–N_3$ and $M–N_6$ bonds, the longer character of the $N_3–O_2$ bond with respect to $N_6–O_7$ and the shorter character of the $N_3–C_4$ bond with respect to $N_6–C_5$. Most of the theoretical bond distances agree with the experimental ones within 0.02 Å. Larger deviations (up to 0.07 Å) can be observed for the M–N and $N_6–O_7$ bonds. A considerable part of the deviations can be attributed to the strong intermolecular interactions in the crystal that appear between the parallel arranged N–O and C=N dipoles and between the

close positioned metals [13–15], this latter being responsible for the found optoelectric properties [7–12].

The data in Table 1 show a trend of Ni–N < Pd–N < Pt–N for the experimental M–N bond distances, while an interchanged order of Pd–N and Pt–N (Ni–N < Pt–N < Pd–N) was obtained in the present computations. The computed slightly longer Pd–N bond with respect to Pt–N agrees with the trend in the ionic radii $Pd^{2+} > Pt^{2+}$ [16], supporting the reliability of the computed data. Furthermore, numerous computed examples are available in the literature for slightly longer bond distances of second-row transition metals compared to those of third-row transition metals in analogous compounds [42]. This phenomenon can be asribed to the stronger relativistic effects in the third-row transition metals contracting several atomic orbitals [43]. The discrepancy between the present computations and the experiment may partly be attributed to slightly different intermolecular interactions in the isomorphous crystals of the two complexes. In addition, the experimental errors for the structural data of [Pd(*dmg*)$_2$] seem to be too small, particularly in the view that Ref. [14] dates 1979. It is more likely that the experimental uncertainty ranges of the close Pd–N and Pt–N bond distances overlap.

The Wiberg bond indices [44] of selected bonds are given in Table 2. They confirm the expected double bond character of the C=N bonds and the partial double bond character of the glyoximic C–C and N–O bonds: that of C–C being the result of the conjugation between the two C=N bonds while that of N–O due to the overlap of the lone pair of O with the π orbital of C=N. Note that the latter overlap is stronger when the oxygen is non-protonated, i.e. O_7 and O_{14}. The weakening of the O–H bonds upon the strong hydrogen bonding interaction are manifested in Wiberg bond indices of around 0.6. The bond indices of the M–N bonds are around 0.4 indicating that these bonds are somewhat weaker than a single bond. This seems to be in contradiction with the M–N distances (computed to be around 1.88, 1.99 and 1.98 Å for M = Ni, Pd and Pt, respectively) being slightly below the sum of the covalent radii of M and N (1.96, 2.06 and 2.03 Å [16], respectively). The contradiction can be solved by considering the ionic contribution in the M–N bonding: A more suitable reference bond distance would be the sum of the ionic radii of the metals (as they are formally M^{2+} ions) and the covalent radius of nitrogen. The M–N distances are considerably higher than these latter reference values (1.38, 1.53 and 1.49 Å [16], respectively) in agreement with the obtained Wiberg indices. For comparison, the formally single Ni–N bond in $Ni(NO)_2$ was computed in the present study to be 1.655 Å with a Wiberg bond index of 0.82.

Table 2
Selected Wiberg bond indices [44] and natural charges in the [M(*dmg*)$_2$] complexes (M = Ni, Pd, Pt)[a]

	[Ni(*dmg*)$_2$]	[Pd(*dmg*)$_2$]	[Pt(*dmg*)$_2$]
M–N_3	0.36	0.38	0.45
M–N_6	0.37	0.39	0.45
N_3–O_2	1.09	1.06	1.06
N_6–O_7	1.24	1.29	1.28
O_2–H_1	0.56	0.62	0.62
$O_7\cdots H_8$	0.20	0.12	0.12
N_3–C_4	1.60	1.60	1.56
N_6–C_5	1.55	1.52	1.49
C_4–C_5	1.09	1.10	1.11
*q*M	+0.75	+0.66	+0.72
qN_3	−0.17	−0.16	−0.18
qN_6	−0.10	−0.06	−0.08
qO_2	−0.53	−0.53	−0.54
qO_7	−0.54	−0.54	−0.54
qH_1	+0.49	+0.51	+0.51

[a] From NBO [31] analysis. The natural charges (*q*) are given in electrons. For numbering of atoms see Fig. 1.

3.2. Hydrogen bonding

The strong O–H···O intramolecular hydrogen bonding is a well-known feature of group 10 [M(*dmg*)$_2$] complexes [45] supported also by the present computations. In agreement with previous conclusion on the basis of IR spectra [22,23], the hydrogen bonding interaction is very strong in [Ni(*dmg*)$_2$] with an H···O distance of ca. 1.4 Å, whereas somewhat weaker in [Pd(*dmg*)$_2$] and [Pt(*dmg*)$_2$] with H···O distances of near 1.6 Å (cf. Table 1). The nature of the O–H···O bond in [Ni(*dmg*)$_2$] has been a debate for some time: early X-ray diffraction and spectroscopic studies suggested a symmetric hydrogen bond [20,25,26]. Other experimental works [13,22,27] and our recent theoretical study [24] proved the asymmetric character of the bond. Similar asymmetric hydrogen bond was found recently in a related amino-oxime Ni(II) complex with O–H and H···O distances of 1.05 Å and 1.43 Å, respectively [46]. The asymmetric nature of the weaker hydrogen bonds in the [Pd(*dmg*)$_2$] and [Pt(*dmg*)$_2$] complexes has been supported by both the previous X-ray diffraction [14,15] and the present computational studies. Note, however, that the asymmetry of the O–H···O hydrogen bonds does not appear pronouncedly in the electronic properties of the O–H···O moiety, as the two oxygens have very close atomic charges (cf. Table 2).

In order to estimate the proton exchange barrier of the OH proton we performed computations on structures with constrained C_{2v} symmetry, that is with a symmetric O···H···O arrangement in which the H···O and O···O distances were allowed to relax. The barriers were determined to be 4.9, 23.0 and 24.9 kJ/mol for the Ni, Pd and Pt complexes, respectively (cf. Table 3). The low barrier found in [Ni(*dmg*)$_2$] can be the reason for the reported disorder (the OH hydrogen placed randomly at one of the oxygens) in its crystal [13]. Both the geometrical parameters and the latter energy data point to very similar hydrogen bonding interactions in [Pd(*dmg*)$_2$] and [Pt(*dmg*)$_2$].

Although the geometrical parameters of O–H···O and its surroundings are also influenced by the metal–ligand donor–acceptor interactions, the well-known effects of hydrogen bonding [47,48] can be recognized in the geomet-

Table 3
Dissociation and proton transfer energies, main charge transfer interactions and the population of the M valence orbitals in the [M(*dmg*)$_2$] complexes (M = Ni, Pd, Pt)[a]

		[Ni(*dmg*)$_2$]	[Pd(*dmg*)$_2$]	[Pt(*dmg*)$_2$]
D_0		2902.3	2982.9	3183.9
ΔE_{barr}		4.9	23.0	24.9
$E^{(2)}$ LP(N_3) → M		438.6	598.4	840.7
$E^{(2)}$ LP(N_6) → M		481.7	769.8	948.4
$E^{(2)}\pi(N_3–C_4)$ → M		26.8	29.3	39.4
$E^{(2)}\pi(N_6–C_5)$ → M		27.6	32.6	40.7
$E^{(2)}\sigma(N_3–O_2)$ → M		13.0	12.0	17.5
$E^{(2)}\sigma(N_6–O_7)$ → M		14.7	15.9	23.4
$E^{(2)}$ M → $\pi^*(N_3–C_4)$		15.1	21.2	35.4
$E^{(2)}$ M → $\pi^*(N_6–C_5)$		15.1	22.1	36.1
Population	*n*s	0.40	0.45	0.63
	(*n*−1)d	8.85	8.88	8.63

[a] From NBO [31] analysis. Energies and second order perturbation energies ($E^{(2)}$ donor → acceptor) in kJ/mol, population of the metal valence orbitals in electron. For numbering of atoms see Fig. 1.

rical data given in Table 1: these are the longer O_2–H_8 bond, the shorter N_3–O_2 and longer N_6–O_7 bonds in the stronger hydrogen-bonded [Ni(*dmg*)$_2$] with respect to the Pd and Pt complexes. The considerable lengthening of the O–H bonds is caused by charge transfer from the proton-acceptor oxygen to the σ^* orbital of the O–H bond [31]. This charge transfer can be characterized by the second-order perturbation energies obtained from Natural Bond Orbital analysis [31], giving values of 303.1, 133.7 and 138.3 kJ/mol for one hydrogen bond in the [Ni(*dmg*)$_2$], [Pd(*dmg*)$_2$] and [Pt(*dmg*)$_2$] complexes, respectively.

The study of the $(dmg)_2^{2-}$ dimer, unperturbed by the donor–acceptor interaction, revealed the nature of the inter-dmg^- hydrogen bonding. According to our computations, a cyclic $(dmg)_2^{2-}$ dimer connected by O–H···O hydrogen bonds is not a stationary point on the potential energy surface! In our various geometry optimizations, starting from this initial $(dmg)_2^{2-}$ structure, two minima were obtained. Note that due to the flexibility of the $(dmg)_2^{2-}$ dimer there are probably additional minima on its potential energy surface, however, a detailed analysis is outside the scope of this study. The most stable cyclic $(dmg)_2^{2-}$ structure presented in Fig. 2 (the other is somewhat twisted and has a higher energy by 7.0 kJ/mol) differs

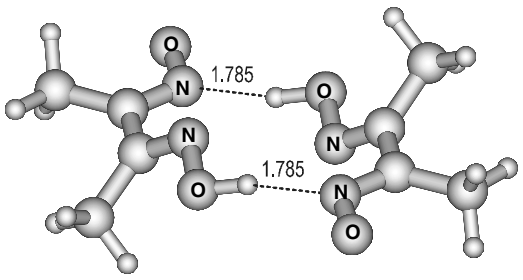

Fig. 2. Relaxed structure of the cyclic $(dmg)_2^{2-}$ ligand. The N···H hydrogen bond distances are given in Å.

considerably from the arrangement of the ligand in the complexes: the two dmg^- moieties are shifted with respect to each other and the O–H···O hydrogen bonds are replaced by O–H···N interactions in the free $(dmg)_2^{2-}$. The length of the H···N hydrogen bonds, 1.785 Å, corresponds to strong interactions. The altered structure of the ligand in the absence of the metal can be attributed to the appearance of strong repulsion effects between the lone pairs of the nitrogens. In the [M(*dmg*)$_2$] complexes the metals act as shields against the repulsion in a way that they localize the lone pairs in the donor–acceptor interactions. On the other hand, computations on a non-cyclic $(dmg)_2^{2-}$ dimer containing only one O–H···O hydrogen bonding interaction resulted in an H···O distance of 1.750 Å, considerably longer than the hydrogen bond lengths in the complexes.

The above results revealed the dominant role of metal–ligand interactions in the title [M(*dmg*)$_2$] complexes. The strong metal–ligand interactions pull the two dmg^- molecules together and facilitate – by binding the nitrogen lone pairs – the strong hydrogen bonding interactions. The hydrogen bond lengths are determined by the metal–ligand distances, i.e., indirectly by the ionic radii of the group 10 elements. Ni with the smallest radius gives the shortest M–N and hydrogen bonds. Accordingly, the larger – and similar – atomic radii of Pd and Pt result in longer M–N and H···O distances (cf. Table 1).

The shorter H···O distances in the complexes as compared to the one in the non-cyclic $(dmg)_2^{2-}$ dimer representing the unperturbed O–H···O interaction mean that the hydrogen bonds are strained in the complexes. The increased repulsion between the OH and O^- groups with respect to a relaxed hydrogen bond is compensated by the donor–acceptor interactions. The hydrogen bonds can still contribute to the total stability of the complexes, particularly in the less strained Pd and Pt complexes. However, this contribution must be a minor one beside the strong metal–ligand interactions.

3.3. Metal–ligand interactions

The title [M(*dmg*)$_2$] complexes are very stable, with energies of dissociation to $M^{2+} + 2\ dmg^-$ of around 3000 kJ/mol (cf. Table 3). These rather high values can be attributed to the very low stability of the resulting ions in vacuum. The dissociation energies increase from M = Ni to Pt. The considerably stronger Pt–N interaction vs. the Pd–N one is in agreement with the slightly shorter computed length of the former bond (cf. Table 1).

The nature of the metal–ligand interactions in the title complexes can be assessed from the natural charges depicted in Table 2. The formally M^{2+} metal ions have natural charges of around +0.7 in these complexes, whereas the charges of the nitrogens are between 0 and −0.2. This points to a considerable charge donation from the ligand to the metals indicating also that the opposite process, the metal-to-ligand backdonation, must be much less.

The above small atomic charges are in agreement with some electrostatic attraction between the metal and nitrogen, playing probably a secondary role beside the donor–acceptor interaction.

In the framework of the Lewis model the following main charge transfer (donor–acceptor) interactions can operate between M^{2+} and the ligand in the title [M(*dmg*)$_2$] complexes:

- σ-donation from the lone pairs (LP) of N to unfilled s and d* valence orbitals of M^{2+}
- σ-donation from the N–O σ bonds to unfilled s and d* valence orbitals of M^{2+}
- π-donation from the π orbitals of N=C double bonds to unfilled d* valence orbitals of M^{2+}
- π-backdonation from occupied d orbitals of M^{2+} to the anti-bonding π* orbitals of N=C bonds

In a HF study of related glyoximate complexes the ligand-to-metal σ-donation was found to be the major component accompanied with minor π contributions [49]. The predominance of the N → M σ-donation in [Ni(*dmg*)$_2$] has also been concluded by Hatsui et al. [29] on the basis of soft X-ray absorption spectroscopy experiments. They found a major peak attributed to σ-donation from the ligand to unfilled 3d* orbitals of Ni and two minor peaks attributed to π-backdonation from M to low-lying π* orbitals of the ligand.

A quantitative assessment of the charge transfer interactions in the title [M(*dmg*)$_2$] complexes (based on the second-order perturbation energies from the NBO analysis) is given in Table 3. The data justify that the main donor–acceptor interaction is the donation from the lone pairs of the nitrogens. The donation is somewhat larger from the nitrogens bonded to the non-protonated oxygens (N_6, N_{13}). This larger donation results in the somewhat smaller negative charge of these nitrogens with respect to the ones bonded to the OH group (N_3 and N_{10}, cf. Table 2). The other charge transfer interactions are weaker by an order of magnitude. The data prove the minor importance of the metal-to-ligand back-donation in the title [M(*dmg*)$_2$] complexes.

The energy contributions of the charge transfer interactions increase generally from [Ni(*dmg*)$_2$] to [Pt(*dmg*)$_2$] parallel with the increase of the dissociation energies (cf. Table 3). According to the second-order perturbation energies, the metal–ligand interactions strengthen more from Pd to Pt than from Ni to Pd. This points to the importance of relativistic effects in the charge transfer interactions, which effects are known to be particularly strong in third-row transition metals. The phenomenon is demonstrated in Fig. 3 using selected orbitals of the Pt^{2+}, Pd^{2+} and $(dmg)_2^{2-}$ fragments. The magnitude of the interaction energy is inversely proportional to the energy difference between the interacting orbitals of the fragments [50]. The stronger relativistic effects in Pt^{2+} stabilize the valence s while destabilize the d orbitals [43] with respect to those in

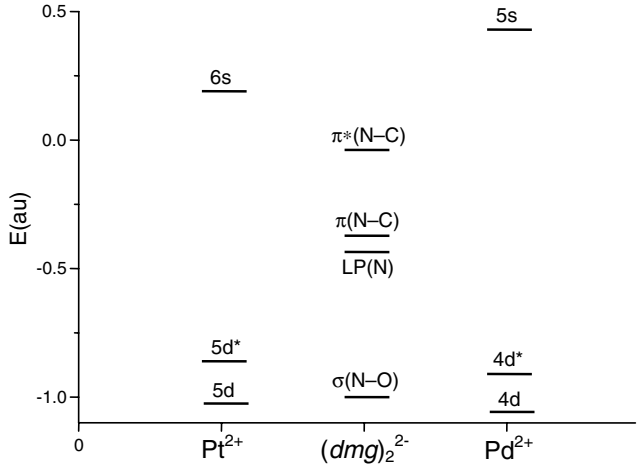

Fig. 3. Energies of selected orbitals of Pd^{2+}, $(dmg)_2^{2-}$ and Pt^{2+} from the NBO analysis.

Pd^{2+}. As appears from the orbital energies depicted in Fig. 3, most donor and acceptor orbitals get closer in energy in [Pt(*dmg*)$_2$] than in [Pd(*dmg*)$_2$]. Particularly the lower energies of the 6s orbitals of Pt^{2+} may contribute significantly to the larger total interaction energy in [Pt(*dmg*)$_2$] indicated by its considerably larger population compared to the 5s orbitals of [Pd(*dmg*)$_2$] (cf. Table 3).

4. Conclusions

We presented here the first systematic theoretical study of bis(dimethylglyoximato) complexes of group 10 transition metals, [M(*dmg*)$_2$], focusing on the hydrogen bonding and metal–ligand interactions. The present computations supported the asymmetric nature of the strong hydrogen bonds and provided the barrier height in the potential energy curve for the proton motion between the two oxygen atoms. However, the strong O$^-$···H–O hydrogen bonding in the cyclic $(dmg)_2^{2-}$ dimer disappears in the absence of the metal atom, which shields the repulsion of the nitrogen lone pairs. Due to this repulsion appearing in the free $(dmg)_2^{2-}$ dimer, the two dmg^- units are shifted from their relative position observed in the complex and the strong O$^-$···H–O interactions are replaced by weaker N···O–H bonds. These results uncover the dominant role of donor–acceptor interactions in the title complexes: the metal–ligand interactions bind the nitrogen lone pairs and make in this way short (but strained) O$^-$···H contacts possible. Consequently, the differences in the radii of the metals determine the differences in the lengths of the hydrogen bonds.

The nature of the bonding interactions between the metals and the $(dmg)_2^{2-}$ ligand was evaluated by Natural Bond Orbital analysis. The computed second-order perturbation energies revealed the predominance of the N → M σ-donation and the secondary importance of the other (π-donation from the N=C bonding orbitals to M, π-backdonation from M to the anti-bonding π* orbitals of the

N=C bonds, σ-donation from the N–O σ orbitals to M) charge transfer interactions. The energy contribution of the donor–acceptor interactions increases from Ni to Pt parallel with the energies of dissociation to $M^{2+} + 2dmg^-$. The trend in the relative stability of the title complexes is in agreement with the importance of relativistic effects in Pt which modify the orbital energies in the favour of donor–acceptor interactions.

Acknowledgements

Computational time from the National Information Infrastructure Development Program of Hungary and support from the Bolyai Foundation and from the Hungarian Scientific Research Foundation (OTKA No. T038189) is gratefully acknowledged.

References

[1] L. Erdey, Gravimetric Analysis, Pergamon Press, Oxford, 1965.
[2] F. Umland, A. Janssen, D. Thierig, G. Wünsch, Theorie und praktische Anwendung von Komplexbildnern, Akademische Verlagsgesellschaft, Frankfurt, 1971.
[3] N. Yoshikuni, T. Baba, N. Tsunoda, K. Oguma, Talanta 66 (2005) 40–44.
[4] B. Fraser, L. Brandt, W.K. Stovall, H.D. Kaesz, S.I. Khan, F. Maury, J. Organomet. Chem. 472 (1994) 317–328.
[5] M. Becht, J. Gallus, M. Hunziker, F. Atamny, K.H. Dahmen, J. Phys. IV 5 (1995) 465–472.
[6] M. Becht, F. Atamny, A. Baiker, K.H. Dahmen, Surf. Sci. 371 (1997) 399–408.
[7] T. Kamata, T. Kodzasa, H. Ushijima, K. Yamamoto, T. Ohta, S. Roth, Chem. Mater. 12 (2000) 940–945.
[8] T. Kamata, T. Kodzasa, H. Ushijima, Colloids Surf. A 198 (2002) 339–345.
[9] I. Shirotani, J. Hayashi, K. Takeda, Mol. Crystallogr. Liq. Crystallogr. 442 (2005) 157–166.
[10] A.A. Dakhel, Y.A.M. Ahmed, J. Phys. Chem. Solids 66 (2005) 1080–1084.
[11] A.A. Dakhel, A.Y. Ali-Mohamed, J. Organomet. Chem. 691 (2006) 3760–3764.
[12] A.A. Dakhel, Y.A.M. Ahmed, F.Z. Henari, Opt. Mater. 28 (2006) 925–929.
[13] D.X. Li, D.J. Xu, Y.Z. Xu, Acta Crystallogr. E 59 (2003) m1094–m1095.
[14] M.S. Hussain, B.E.V. Salinas, E.O. Schlemper, Acta Crystallogr. B 35 (1979) 628–633.
[15] M. Konno, T. Okamoto, I. Shirotani, Acta Crystallogr. B 45 (1989) 142–147.
[16] WebElements™, the periodic table on the WWW, http://www.webelements.com.
[17] R.E. Rundle, M. Parasol, J. Chem. Phys. 20 (1952) 1487.
[18] A. Nakahara, Bull. Chem. Soc. Japan 28 (1955) 473.
[19] R. Blinc, D. Hadži, J. Chem. Soc. (1958) 4536.
[20] J.E. Caton Jr., C.V. Banks, Inorg. Chem. 6 (1967) 1670.
[21] A. Bigotto, G. Costa, V. Galasso, G. De Alti, Spectrochim. Acta 26A (1970) 1939.
[22] B. Orel, M. Penko, D. Hadži, Spectrochim. Acta 36A (1980) 859.
[23] P.K. Panja, S. Bala, C. Pal, P.N. Ghosh, J. Mol. Struct. 249 (1991) 277.
[24] A. Szabó, A. Kovács, J. Mol. Struct. 651-653 (2003) 547–553.
[25] L.E. Godycki, R.E. Rundle, Acta Crystallogr. 6 (1953) 487.
[26] E. Frasson, C. Panattoni, R. Zannetti, Acta Crystallogr. 12 (1959) 1027–1031.
[27] D.E. Williams, G. Wohlauer, R.E. Rundle, J. Am. Chem. Soc. 81 (1959) 755–756.
[28] D.M. Adams, D.C. Stevens, Inorg. Chem. 20 (1981) 525.
[29] T. Hatsui, Y. Takata, K. Kosugi, K. Yamamoto, T. Yokoyama, T. Ohta, J. Electron Spectrosc. Relat. Phenom. 88-91 (1998) 405–409.
[30] L.G.M. Pettersson, T. Hatsui, N. Kosugi, Chem. Phys. Lett. 311 (1999) 299–305.
[31] A.E. Reed, L.A. Curtiss, F. Weinhold, Chem. Rev. 88 (1988) 899.
[32] A.D. Becke, J. Chem. Phys. 98 (1993) 5648.
[33] C. Lee, W. Yang, R.G. Parr, Phys. Rev. B 37 (1988) 785.
[34] P.J. Hay, W.R. Wadt, J. Chem. Phys. 82 (1985) 299.
[35] A.W. Ehlers, M. Böhme, S. Dapprich, A. Gobbi, A. Höllwarth, V. Jonas, K.F. Köhler, R. Stegmann, A. Veldkamp, G. Frenking, Chem. Phys. Lett. 208 (1993) 111.
[36] J.P. Perdew, Phys. Rev. B 33 (1986) 8822.
[37] S.F. Boys, F. Bernardi, Mol. Phys. 19 (1970) 553.
[38] M.J. Frisch, G.W. Trucks, H.B. Schlegel, G.E. Scuseria, M.A. Robb, J.R. Cheeseman, J.A. Montgomery Jr., T. Vreven, K.N. Kudin, J.C. Burant, J.M. Millam, S.S. Iyengar, J. Tomasi, V. Barone, B. Mennucci, M. Cossi, G. Scalmani, N. Rega, G.A. Petersson, H. Nakatsuji, M. Hada, M. Ehara, K. Toyota, R. Fukuda, J. Hasegawa, M. Ishida, T. Nakajima, Y. Honda, O. Kitao, H. Nakai, M. Klene, X. Li, J.E. Knox, H.P. Hratchian, J.B. Cross, V. Bakken, C. Adamo, J. Jaramillo, R. Gomperts, R.E. Stratmann, O. Yazyev, A.J. Austin, R. Cammi, C. Pomelli, J.W. Ochterski, P.Y. Ayala, K. Morokuma, G.A. Voth, P. Salvador, J.J. Dannenberg, V.G. Zakrzewski, S. Dapprich, A.D. Daniels, M.C. Strain, O. Farkas, D.K. Malick, A.D. Rabuck, K. Raghavachari, J.B. Foresman, J.V. Ortiz, Q. Cui, A.G. Baboul, S. Clifford, J. Cioslowski, B.B. Stefanov, G. Liu, A. Liashenko, P. Piskorz, I. Komaromi, R.L. Martin, D.J. Fox, T. Keith, M.A. Al-Laham, C.Y. Peng, A. Nanayakkara, M. Challacombe, P.M.W. Gill, B. Johnson, W. Chen, M.W. Wong, C. Gonzalez, J.A. Pople, GAUSSIAN 03, Gaussian Inc., Wallingford CT, 2004.
[39] E.D. Glendening, J.K. Badenhoop, A.E. Reed, J.E. Carpenter, J.A. Bohmann, C.M. Morales, F. Weinhold, NBO 5.0, Theoretical Chemistry Institute, University of Wisconsin, Madison, 2001.
[40] M.J. Frisch, G.W. Trucks, H.B. Schlegel, G.E. Scuseria, M.A. Robb, J.R. Cheeseman, V.G. Zakrzewski, J.A. Montgomery Jr., R.E. Stratmann, J.C. Burant, S. Dapprich, J.M. Millam, A.D. Daniels, K.N. Kudin, M.C. Strain, O. Farkas, J. Tomasi, V. Barone, M. Cossi, R. Cammi, B. Mennucci, C. Pomelli, C. Adamo, S. Clifford, J. Ochterski, G.A. Petersson, P.Y. Ayala, Q. Cui, K. Morokuma, A.D. Rabuck, K. Raghavachari, J.B. Foresman, J. Cioslowski, J.V. Ortiz, B.B. Stefanov, G. Liu, A. Liashenko, P. Piskorz, I. Komaromi, R. Gomperts, R.L. Martin, D.J. Fox, T. Keith, M.A. Al-Laham, C.Y. Peng, A. Nanayakkara, C. Gonzalez, M. Challacombe, P.M.W. Gill, B. Johnson, W. Chen, M.W. Wong, J.L. Andres, C. Gonzalez, M. Hcead-Gordon, E.S. Replogle, J.A. Pople, GAUSSIAN 98, Gaussian Inc., Pittsburgh PA, 1998.
[41] G. Schaftenaar, Molden 3.8, CAOS/CAMM Center Nijmegen, Nijmegen, The Netherlands, 2003.
[42] G. Frenking, I. Antes, M. Böhme, S. Dapprich, A.W. Ehlers, V. Jonas, A. Neuhaus, M. Otto, R. Stegmann, A. Veldkamp, S.F. Vyboishchikov, in: K.B. Lipkowitz, D.B. Boyd (Eds.), Reviews in Computational Chemistry, VCH, New York, 1996, pp. 63–143.
[43] M. Dolg, in: P.v.R. Schleyer, N.L. Allinger, T. Clark, J. Gasteiger, P.A. Kollman, H.F. SchaeferIII, et al. (Eds.), Encyclopedia of Computational Chemistry, Wiley, Chichester, 1998, pp. 1478–1486.
[44] K.B. Wiberg, Tetrahedron 24 (1968) 1083.
[45] K. Nakamoto, Infrared and Raman Spectra of Inorganic and Coordination Compounds. Part B: Applications in CoordinationOrganometallic and Bioinorganic Chemistry, Wiley, New York, 1997.
[46] G. Tauzher, R. Dreos, A. Felluga, G. Nardin, L. Randaccio, M. Stener, Inorg. Chim. Acta 355 (2003) 361–367.
[47] A. Kovács, V. Izvekov, K. Zauer, K. Ohta, J. Phys. Chem. A 105 (2001) 5000–5009.
[48] A. Kovács, A. Szabó, I. Hargittai, Acc. Chem. Res. 35 (2002) 887.
[49] S. Di Bella, M. Casarin, I. Fragala, G. Granozzi, T.J. Marks, Inorg. Chem. 27 (1988) 3993–4002.
[50] T.A. Albright, J.K. Burdett, M.-H. Whangbo, Orbital Interactions in Chemistry, Wiley, New York, 1985.